

## Electrochemical Performance of Starch-Polyaniline Nanocomposites Synthesized By Sonochemical Process Intensification

Narsimha Pandi<sup>1</sup>, Shirish H. Sonawane<sup>1,\*</sup>, Sarang P. Gumfekar<sup>2</sup>, Anand Kishore Kola<sup>1</sup>, Pramod H. Borse<sup>3</sup>, Swapnil B. Ambade<sup>4</sup>, Sripath Guptha<sup>1</sup> and Muthupandian Ashokkumar<sup>5</sup>

<sup>1</sup>Department of Chemical Engineering, National Institute of Technology, Warangal, Telangana, India.

<sup>2</sup>Department of Chemical and Materials Engineering, University of Alberta, Edmonton, Canada.

<sup>3</sup>International Advanced Research Centre for Powder Metallurgy and New Materials, Balapur PO, Hyderabad, Telangana, India.

<sup>4</sup>Department of Organic and Nano Engineering, Hanyang University 222, Wangsimni-ro, Seongdong-gu, Seoul, Korea.

<sup>5</sup>Department of Chemistry, University of Melbourne, Victoria, Australia.

\*Corresponding Author: Shirish H. Sonawane. Email: shirish@nitw.ac.in.

**Abstract:** The present study deals with the intensified synthesis of starch-polyaniline (starch-PANI) nanocomposite using an ultrasound-assisted method. Starch is a key component in this nanocomposite, which acts as a backbone of the nucleation of PANI. The Electrochemical property of the nanocomposite arises due to the addition of PANI. This is one of green approach for the synthesis of bio nanocomposite using ultrasound. The crystallinity of the composite is evaluated using the Scherrer Formula. The starch-PANI nanocomposite was characterized by XRD, FT-IR, Raman, XPS and TEM. The composite nanoparticles show spherical morphology. The elemental composition of starch-PANI showed O 1s peak at 546 eV, N 1s peak at 416 eV, C 1s peak at 286 eV and S 1s peak at 176 eV. The electrochemical studies of the starch-PANI electrodes are evaluated by cyclic voltammetry (CV), galvanostatic charge/discharge (GCD), and electrochemical impedance spectroscopy (EIS). Starch-PANI electrode has shown the maximum specific capacitance of 499.5 F/g at 5 mV/s scan rate.

**Keywords:** Starch; polyaniline; sonochemical synthesis; ultrasound; biocomposite; electrochemical analysis; supercapacitor

### 1 Introduction

This era marks the rising demand for energy storage in industrial, electronics, and automobile applications. High power and energy density, short time charge-discharge and longer life cycle, are the attributes that make supercapacitors a reliable source for energy generation and storage [1]. Because of their enormous applications and uses, supercapacitors are filling the gap between batteries and capacitors [2]. The important behavior of the supercapacitors is that they cannot only discharge in a short period but also charged in a very short period. Depending on their charge storage mechanism, electrochemical capacitors can be broadly divided into electric double-layer capacitors (EDLCs), pseudocapacitors and hybrid capacitors [3,4]. Generally, carbon-based materials are used to fabricate electrodes in EDLCs because of their high rates of absorption/desorption of electrolytic ions [4]. The pseudocapacitors store charges through the Faradaic process. In pseudocapacitors metal oxides, porous carbon-based composites and the polymer composites are used as electrode materials [5]. On the contrary, the hybrid capacitor consists of a battery type electrode (Faradaic) and capacitive type electrode (electrostatic), resulting in high power and energy densities [5].

Starch is a polysaccharide, which is mainly extracted from natural sources and consists of amylose and amylopectin. Carbon derivatives extracted from starch have proved to be a promising source for electrochemical applications [6,7]. In the past, porous carbon and carbon microspheres were extracted

from starch and used for supercapacitor electrode applications [8,9]. Starch and cellulose are chemically similar, since these polymers are made of repeating glucose monomers and only differ in their geometric configuration. There is extensive work reported on the cellulose composite's electrode materials for supercapacitors. Libo et al. [10] reported that the synthesis of cellulose/CNT nanofibers for supercapacitor electrodes and have shown better microstructural and enhanced electrical properties. Few attempts reported on utilization cellulose/polyaniline [11], nanocellulose/polypyrrole [12] composites for electrochemical applications. These reports mainly focused on tapping the electrolyte absorption and energy deposition properties that cellulose has to offer [13]. There has been no extensive research carried out on the use of starch composites for applications in supercapacitors, though certain composites as starch/graphene [14], starch-polymer/metal oxide are promising materials for electrochemical applications [14,15].

Intrinsically conducting polymers (ICP) are organic macromolecules having special conducting properties viz polyaniline (PANI), polypyrrole, polythiophene and polyacetylene are few well known systems. PANI and polypyrrole composites have been extensively explored for the supercapacitor electrode applications [1,16,17]. PANI was extensively used to prepare the composites with graphene [18], carbon nanotubes [19,20], carbon paper [21], gold [22], stainless steel [23], graphite [24,25], activated carbon [26] due to its easy synthesis and deposition. It is important to mention that PANI offers high pseudocapacitive performance. Eftekhari et al. showed that they observed an increased specific capacitance when PANI was deposited on carbon and metal oxide-based templates [27]. Based on this, PANI-graphene [28], PANI-SnO<sub>2</sub> [29], PANI-MnO<sub>2</sub> [30] and ternary composites PANI-graphene-carbon nanotubes (CNT) [31], MnO<sub>2</sub>-PANI-reduced graphene oxide [32] have been reported for giving high specific capacitance.

Previous work has shown the preparation of PANI/biopolymer composites using various matrices which include chitosan, cellulose and cellulose derivatives [33]. A few reports have studied on the usage of starch as a biopolymer for the above mentioned PANI/biopolymer composites. PANI deposited on non-toxic, biodegradable starch can lead to the formation of nanocomposites for various electrochemical applications [33]. Ehsan et al. [34] reported on an enhanced thermal and mechanical characteristics of PANI/Starch/polystyrene composites. Yuhong et al. [1] discussed the preparation of rGO/PANI/SnO<sub>2</sub> nanocomposite for supercapacitance and reported high supercapacitance and good cycling stability. There are a very few studies on the synthesis and application of starch-PANI composites for energy generation and storage applications.

In this work, we have used sonochemical routes for synthesizing the nanocomposites. The chemical effects caused by ultrasound energy (acoustic waves) are mainly because of the cavitation effects [35]. Process intensification using ultrasound has been previously reported for the synthesis of platinum-ruthenium [36], gold and platinum nanoparticles [37] for use in fuel cells as electrodes. Researchers also synthesized Cu<sub>2</sub>O-graphene [38], and graphene oxide-Fe<sub>2</sub>O<sub>3</sub> [39] using process intensification for lithium ion battery electrodes. Dipanwita et al. [40] and Shahram et al. [41] reported that the synthesis of MnO<sub>2</sub>-graphene composites by using sonochemical method, which gave good specific capacitance and cyclic stability. Ultrasound assisted synthesis aids in the preparation of uniformly distributed nanoparticles in a very short time and utilizing less energy. High reaction rates can be achieved using sonochemistry, resulting in time efficient synthesis. Sonochemical method is an energy and time efficient technique, when compared to other methods viz. solvothermal, electrochemical and microwave [42].

Cavitation will help to prepare the starch-PANI nanocomposite and also due to the cavitation effect conductivity nature of the composite enhanced. Nazarzadehzareh E et al. [30] discussed the preparation of starch-PANI nanocomposite by ultrasonic irradiation and reported that conductivity of the composite enhanced by ultrasound are mainly because of the cavitation effects and also they found that conductivity of the composite was increased by increasing the polyaniline. Ultrasound assisted synthesis of starch-PANI procedure as follows, initially 100 mL of 1 M HCl added in 250 mL beaker followed by 4 mL of aniline was added. Then 3 g starch was added into the above mixture and sonicated for 30 min. Following sonication 5 g APS solution dropwise added to the above solution and sonicated in ice bath for 1 h. Then the above resultant mixture was kept under ultrasound probe sonication in ice bath further 6 h to

completion of polymerization. After completion of sonication, starch-PANI powder was obtained through repeated filtration, washing with deionized water and methanol. The resultant product was dried in vacuum at 50°C.

In this work, we have used an ultrasound assisted method for synthesizing the starch-PANI nanocomposites for supercapacitor. Aniline was polymerized on the conductive surface of starch granules in the presence of CTAB. APS was used as an initiator for polymerization. The specific capacitance was mainly contributed from the pseudo capacitance from the addition of polyaniline. Finally, we have synthesized starch-PANI nanocomposite and achieved high reaction rates at less time period. The structural parameters, functional groups and morphology of the synthesized nanocomposite were studied in detail. The electrochemical studies of the nanocomposite calculated by using CV, GCD and EIS. A few reports have studied on the preparation of starch-PANI nanocomposite and its electrochemical applications. W. Wu et al. [51] discussed the preparation of the pure PANI, G-PANI and SDAS-PANI with their specific capacitances were 237, 379 and 433 F/g, respectively which are lower than present work starch-PANI specific capacitance is 499.5 F/g. Several reports are studied on the synthesis of starch-PANI, but those reports are various methods for different applications. According to the previous literature till date, no reports on electrochemical properties of starch-PANI nanocomposite, especially supercapacitor application.

Ultrasound cavitation is one of a green approach to use for nanocomposite synthesis. The use of ultrasound energy is greater interest in the area of green chemistry for synthesis. In this work ultrasound irradiation is used for formation of bio nanocomposite. Nowadays, food waste is a major issue. There is a need to convert these food wastes into useful materials. Generally, starch can be extracted from food waste and used for synthesis of various composites. Starch is an environmentally friendly and biodegradable material. In view of this issue, the current reports deal with ultrasound assisted synthesis of starch-PANI nanocomposite. The crystalline size, morphology, functional groups and elemental compositions were analyzed. Electrochemical studies of starch-PANI electrodes for supercapacitor were calculated by CV, GCD, and EIS. The specific capacitance of composite material was also investigated.

## 2 Experimental

### 2.1 Materials

Starch, sulfuric acid ( $\text{H}_2\text{SO}_4$ , 98 wt%), aniline (99%) were procured from Zen Chemicals, Bangalore, India, ammonium persulfate (APS) (98%) and cetyltrimethylammonium bromide (CTAB) were procured from Sisco Research Laboratories Pvt Ltd., Mumbai, India. Deionized water was used to prepare the all aqueous solutions. All other chemicals and solvents were used as received.

### 2.2 Method

#### 2.2.1 Sonochemical Synthesis of Starch-PANI Nanocomposite

The starch-PANI nanocomposite was synthesized using sonochemical method. Fig. 1 shows the schematic representation of nanocomposite synthesis. Initially, 5 g of starch was added in 250 mL of deionized water to which 0.15 g of CTAB was added. Then the mixture was sonicated for 30 min by using a 20 kHz ultrasound probe sonicator (2 s on 1 s off time pulse mode, M/s Dakshin Ultrasonicator, Mumbai, India, tip diameter 10 mm, Fig. 2). Following sonication 2 mL of 98%  $\text{H}_2\text{SO}_4$  was added to the sonicated solution, and the ultrasound-assisted acid hydrolysis led to the formation of starch nanocrystals. To this solution 2.5 g of aniline was added and sonicated for 30 min. 0.5 g ammonium per-sulphate initiator was added to the solution by dropwise and sonicated in an ice bath for 30 min, at a constant temperature of 10°C. Miniemulsion of aniline was formed using addition of CTAB. The starch-PANI nanocomposite was obtained through repeated filtration, washing with deionized water and ethanol. The resultant compound was dried in a vacuum oven at 80°C for 6 h. Fig. 3 shows the procedural flow of the synthesis.

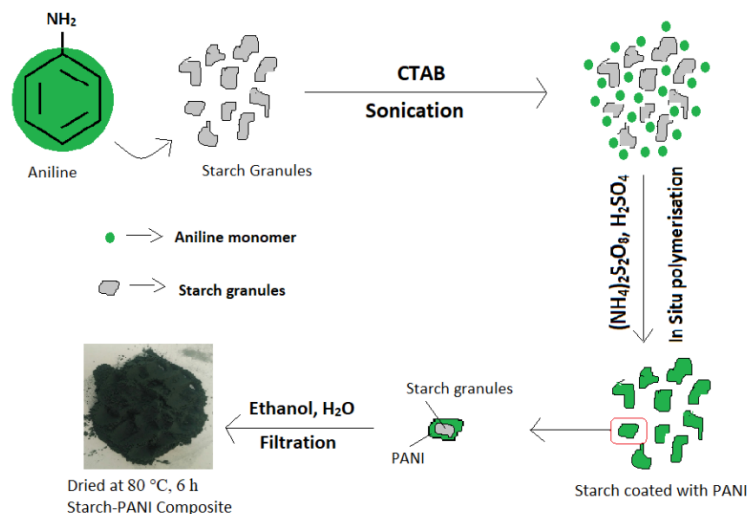


**Figure 1:** Graphical representation of starch-PANI nanocomposite synthesis using sonochemical method

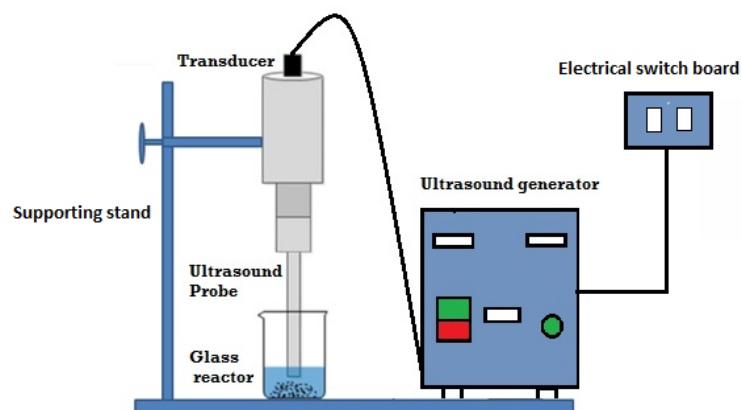


**Figure 2:** Ultrasound set up for the synthesis of starch-PANI composite

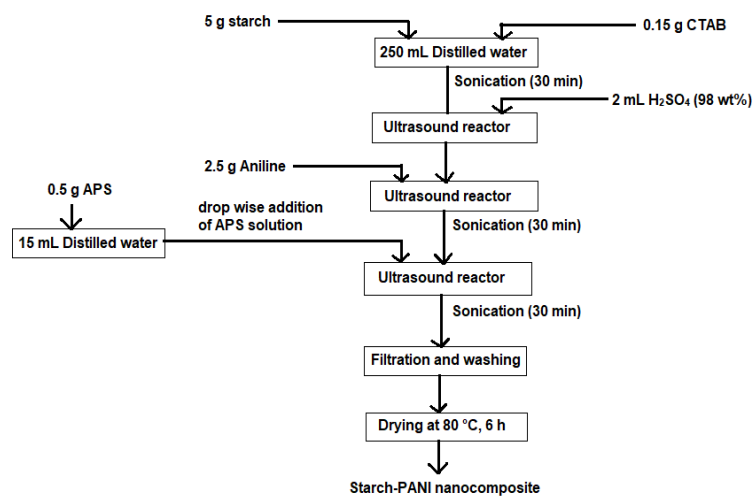


**Figure 3:** Procedural flow of the synthesis of starch-PANI nanocomposite

### 2.3 Characterization Methods

X-ray Diffraction (XRD) spectra were recorded on a Bruker D8 Advanced X-ray diffractometer. Fourier Transform Infrared Spectroscopy (FTIR) spectra were recorded using KBr pellet method by PerkinElmer Spectrum 100 FTIR spectrophotometer. Transmission electron microscope (TEM) analysis was performed by Philips CM 200. Raman spectra were recorded by inVia, Renishaw Raman microscope (Renishaw, UK) and X-ray photoelectron spectroscopy (XPS) were carried out by ESCALab 2000 system, Thermo Scientific, USA.

### 2.4 Electrochemical Characteristics

Electrochemical performance of supercapacitor was conducted using 3 electrode system consisting of 1 M Na<sub>2</sub>SO<sub>4</sub> aqueous solution, wherein starch-PANI coated carbon paper was used as working electrode, graphite plate as counter electrode and standard saturated calomel electrode (SCE) as reference electrode. The working electrode for electrochemical measurement was made by mixing the synthesized material (starch-PANI composite), carbon black and polyvinylidene fluoride (PVDF) in mortar and pestle with the mass ratio of 75:20:5 and adding few drops of N-methyl-2-pyrrolidinone (NMP) to form uniform slurry. The resultant mixture was coated on a carbon paper (1 cm × 1 cm) and dried at vacuum oven.

Electrochemical performance of electrochemical capacitor was carried out by CV, GCD, and EIS methods by using a PARSTAT 2273 (Advanced Electrochemical System) testing system. CV and GCD were evaluated in the potential range of -0.2 to +0.8 V at various scan rates varying from 5 to 160 mV/s and various current densities (0.5, 1 and 2 A/g). The electrochemical impedance spectroscopic (EIS) measurement was evaluated at 0.1-1 × 10<sup>5</sup> Hz as frequency range and voltage amplitude 5 mV.

## 3 Results and Discussion

### 3.1 XRD Analysis

The phase structure and the crystallite size of starch-PANI composite were elucidated using the XRD analysis. The observed peaks at 2 $\Theta$  = 17.24°, 23.18° and 30.50° which associated with (200), (211) and (311) planes of the starch, respectively while at 15.24°, 18.16°, 20.04° and 26.60° which associated with (011), (100), (020) and (200) planes of the PANI, respectively [34,43]. Bouget et al. [44] have discussed in detail the structural parameters of polyaniline by in situ polymerization and indicating pseudoorthorhombic crystallite structure form. The XRD results are in line with the previous observations reflecting highly ordered crystallite structure of starch-PANI composite. Due to the effect of ultrasound the crystallite size of the Starch-PANI nanocomposite was smaller in size. Individually starch is not crystalline material. However, crystallinity bring out by using addition of polyaniline in the composite using ultrasound. In XRD, identified the starch interference in the composite as shown in Fig. 4. Structural parameters of as synthesized starch-PANI nanocomposite results are tabulated in Tab. 1. The crystallite size of composite was evaluated by Scherrer Formula [45].

$$L_p = \frac{0.94\lambda}{\beta_{1/2} \cos\theta} \quad (1)$$

where

L<sub>p</sub> = Average Crystallite size,

B = Full width at half maximum,

$\theta$  = Bragg angle

$\lambda$  = X-ray wavelength

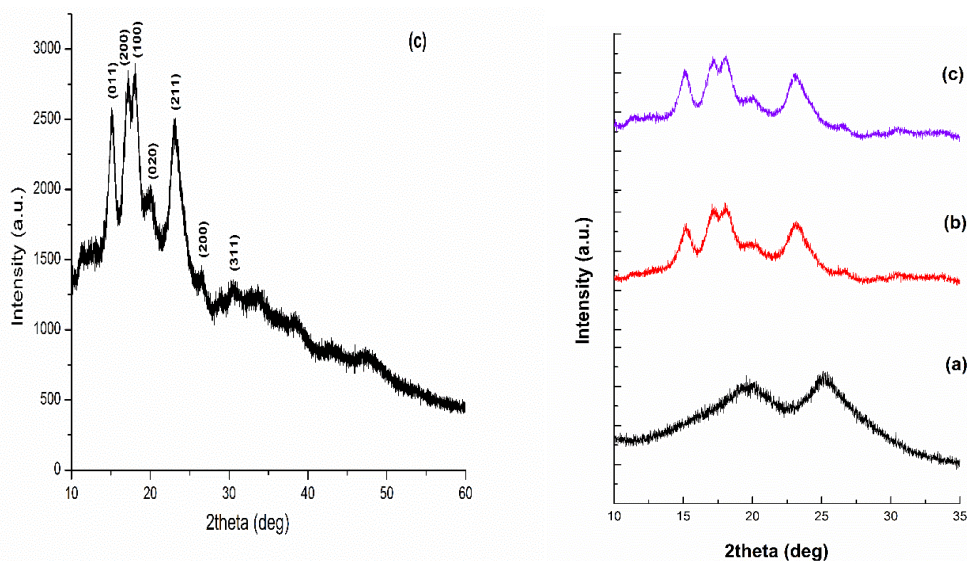


**Figure 4:** XRD pattern of starch-PANI nanocomposite:(a) PANI, (b) Starch and (c) Starch-PANI

**Table 1:** Structural parameters obtained from XRD of synthesized starch-PANI nanocomposite

No.	2 $\theta$ (Degree)	(h k l) plane	Components	d-spacing ( $\text{\AA}$ )	FWHM	Crystallite Size (nm)
1	15.24	(011)	PANI	5.80	0.34	24.63
2	17.24	(200)	Starch	5.13	0.25	33.33
3	18.16	(100)	PANI	4.77	0.44	19.11
4	20.04	(020)	PANI	4.40	0.18	46.83
5	23.18	(211)	Starch	3.86	0.09	89.67
6	26.60	(200)	PANI	3.35	0.26	33.86
7	30.50	(311)	Starch	2.93	0.62	13.66

### 3.2 FTIR Analysis

FTIR is used to identify the functional groups present in starch-PANI composite. The characteristic broad peak of starch ( $3370.63\text{ cm}^{-1}$ ) and PANI ( $1639.93$ ,  $1461.85$ ,  $1162.68$  and  $785.41\text{ cm}^{-1}$ ) are observed in the synthesized starch-PANI composite. The structural and functional groups of starch and PANI are also reported in the literature [46,47]. The characteristic broad band peak at  $3370.63\text{ cm}^{-1}$  attributed to O-H group indicates starch. A peak at  $2926.14\text{ cm}^{-1}$  can be attributed to C-H band stretching vibration of pyranoid ring. The broad band peak at  $1639.93\text{ cm}^{-1}$  can be assigned as N-H bending, and those at  $1461.85$ ,  $1421.36$  and  $1340.65\text{ cm}^{-1}$  could be assigned to C-C stretching vibration for benzenoid ring. The broad band peaks at  $1244.09$  and  $929.84\text{ cm}^{-1}$  are due to C-N and C-H stretching vibrations of the aromatic ring, respectively. Further, the spectrum exhibits the presence of aromatic ( $860.51$ ,  $764.82$  and  $709.13\text{ cm}^{-1}$ ) and carboxyl ( $1244.09\text{ cm}^{-1}$ ), alkane ( $527.61\text{ cm}^{-1}$ ) groups from PANI and starch. Several other bonds such as C-O-C and C-O are observed as broad bands between  $1244.09$ - $860.51\text{ cm}^{-1}$ . The FTIR analysis for starch and polyaniline included, which are shown in Fig. 5. It can see that starch-PANI nanocomposite formed and which are line with the previous studies [29,48].

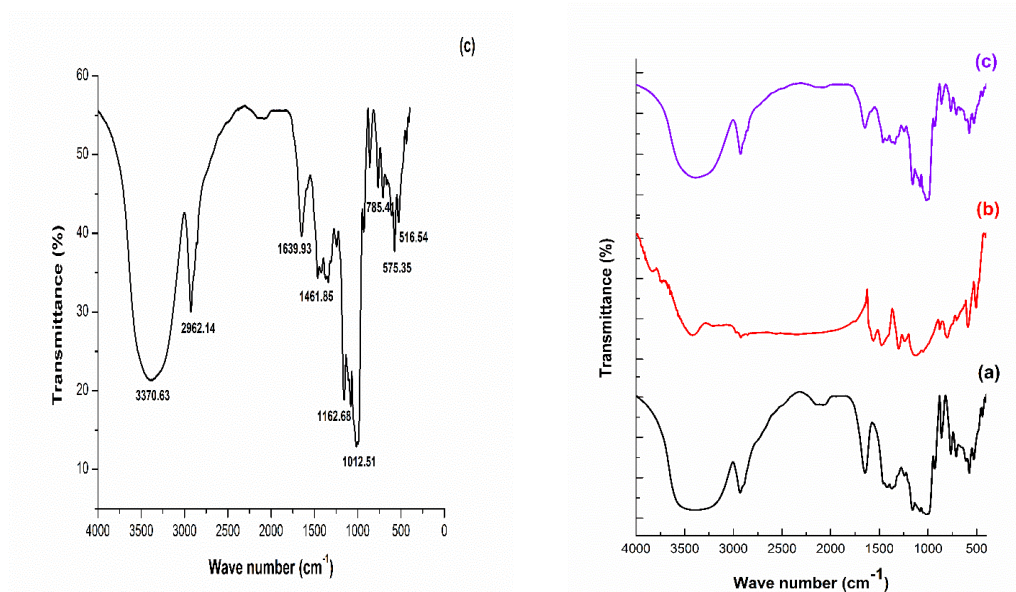


**Figure 5:** FT-IR spectra of synthesized starch-PANI nanocomposite:(a) Starch, (b) PANI and (c) Starch-PANI

### 3.3 TEM Analysis

The images of starch-PANI nanocomposite were obtained from transmission electron microscopy (TEM) analysis (Fig. 6). The composite nanoparticles show spherical shape and closely bound with the surface of starch. Due to the polymerization of aniline, surface of the particles is rough in nature, giving a better conductivity for the electrode material. The average particle size of the starch-PANI composite was approximately 20-100 nm.

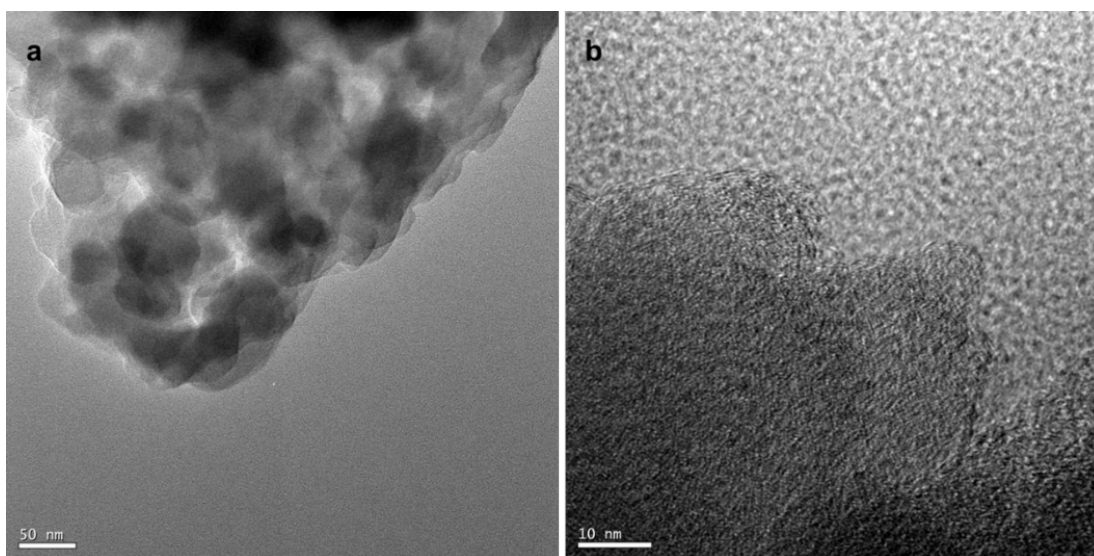


**Figure 6:** Morphology of synthesized starch-PANI composite (a) 50 nm and (b) 10 nm by Sonochemical method

### 3.4 Raman Spectroscopy Analysis

Raman spectral analysis (Fig. 7) was used to obtain structural information of the PANI based composite material. The bands between 818 cm<sup>-1</sup> and 1236 cm<sup>-1</sup> which are attained with C-H bending

modes, between  $1547\text{ cm}^{-1}$  and  $1610\text{ cm}^{-1}$  to stretching modes of C-C, and various C-N stretching modes (polarons, amines, imines) between  $1236\text{ cm}^{-1}$  and  $1547\text{ cm}^{-1}$ . A weak band at  $1180\text{ cm}^{-1}$  can be assigned to C-C bond in plane deformation of quinoid ring of the PANI. The bands at  $1337\text{ cm}^{-1}$ ,  $1411\text{ cm}^{-1}$ , and  $1610\text{ cm}^{-1}$  are attributed to C-N stretching, C-C stretching of benzamide and benzide units, respectively. The intense bands at  $1180\text{ cm}^{-1}$  and  $1610\text{ cm}^{-1}$  are characteristic of p-disubstituted benzene rings. Few weak bands are observed at  $1411\text{ cm}^{-1}$ ,  $1337\text{ cm}^{-1}$ , and  $1236\text{ cm}^{-1}$  due to the formation of semiquinone radical cations, which are, p-disubstituted benzene which were further converted to polarons [19].

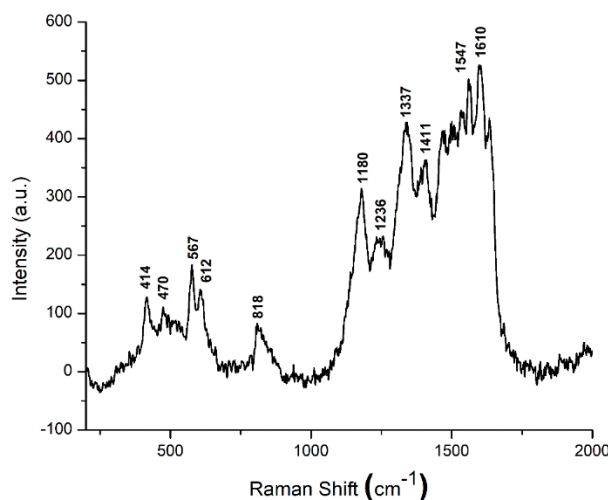


**Figure 7:** Raman spectra of synthesized starch-PANI nanocomposite

### 3.5 XPS Analysis

The surface analysis and elemental composition of starch-PANI composites was carried out using XPS and presented in (Fig. 8). The XPS spectrum of the composite showed peaks for O 1s at 546 eV, N 1s at 416 eV, C 1s at 286 eV and S 1s at 176 eV [49]. The presence of sulphur is due to sulphate formed from ammonium per sulphate.

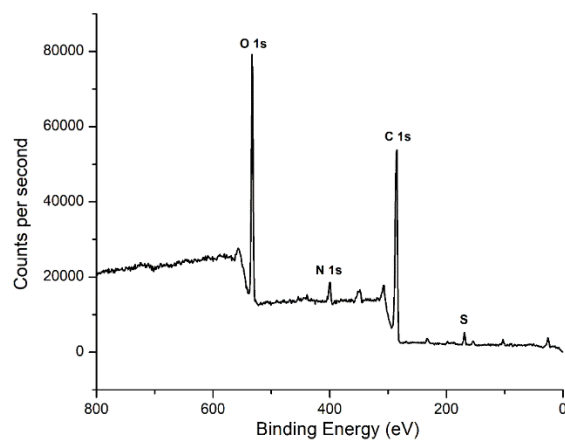


**Figure 8:** X-ray photoelectron spectra (XPS) of starch-PANI nanocomposite

The individual elements of XPS spectra were analyzed to understand the composition. The N 1s plot is shown in Fig. 9(a), the composite was deconvoluted into three sub-peaks for -NH-,  $\text{N}^+/\text{N}$ , and  $\text{N}=\text{N}$  at 399 eV, 400.3 eV, and 402.2 eV respectively. The area under the graph indicates that the -NH- is present in the highest quantity. The  $\text{N}^+$  is observed due to the presence of protonated emeraldine base

form of PANI. The starch and  $N^+$  could possibly result in the formation of hydrogen bonds. The C 1s scan is shown in the Fig. 9(b), the higher intensity peak at 284.4 eV can be attributed to C-OH, other peaks for (C-H, C-C), C=O, and C-N are found at 286.4 eV, 287.9 eV, and 289 eV respectively. The O 1s XPS spectra in Fig. 9(c) show three subplots at 532.7 eV, 534.6 eV and 530.9 eV representative of -C-OH, S-O and C-OC bonding states respectively [49,50].

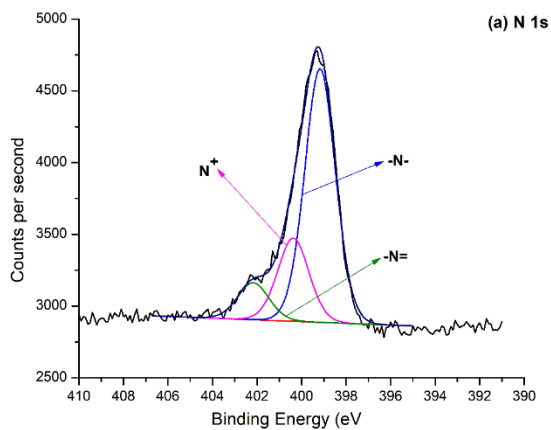


**Figure 9:** (a) XPS spectra of N 1s for starch-PANI

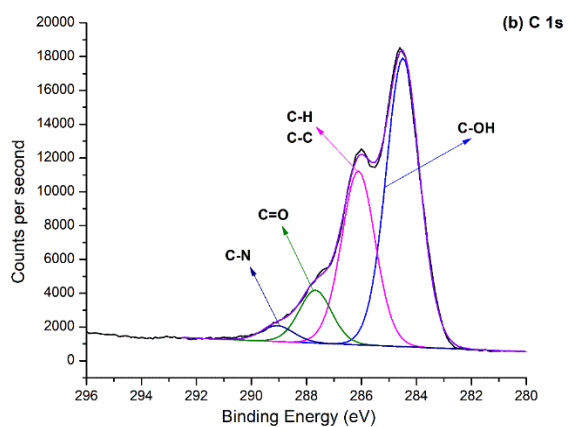


**Figure 9:** (b) XPS spectra of C 1s for starch-PANI

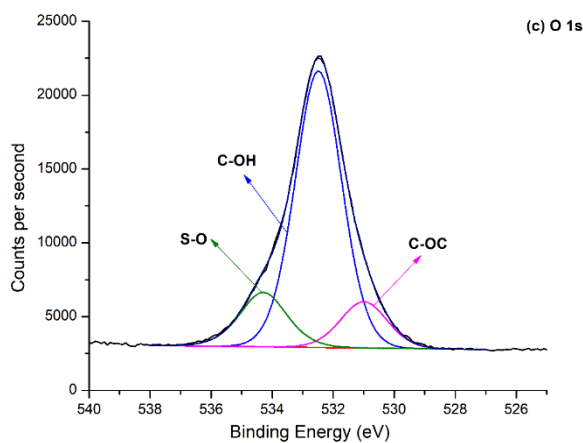


**Figure 9:** (c) XPS spectra of O 1s for starch-PANI

### 3.6 Electrochemical Analysis

Starch-PANI composite electrode and its electrochemical studies of supercapacitors were characterized by using CV, GCD, and EIS analysis are conducted in a three-electrode system with 1M Na<sub>2</sub>SO<sub>4</sub> electrolyte solution.

#### 3.6.1 Cyclic Voltammetry (CV)

Fig. 10 shows the CV measurements in 1 M Na<sub>2</sub>SO<sub>4</sub> electrolyte solution at different scan rates varying from 5 to 160 mV/s for starch-PANI composite. It can be observed that curves are quasi rectangular shape at 40, 80 and 160 mV/s and curves shapes are steady with the increasing scan rate, which represent that good electrochemical capacitive behavior of the prepared electrodes. But few oxidative peaks at scan rates of 5, 10 and 20 mV/s, which indicates the EDLC behavior. Area under CV curves are proportional with the capacitance and curves are almost similar shape, which shows the mirror characteristics, which indicates that redox reactions are electrochemically reversible and also electrochemical capacitor behavior [4]. Previous literature has shown that curves of PANI and PANI based composite. K.Z. Htut et al. [55] reported that the CV curves show two redox peaks for each oxidation and reduction process for PANI and PANI based composites, which can be assign to the conducting state (emeraldine/permigraniline) and semiconductor state (leucoemeraldine/emeraldine) transitions of PANI. A. Alptekin et al. [56] reported that CV curves of VACNT/PANI at different scan rates and found that area under the curve increases with the increasing the scan rates from 20 to 400 mV/s and oxidation peaks to be steady on the CV curve and its indicates resistance effects were not pronounced for the synthesized composite electrodes, otherwise CV curves shape from horizontal to diagonal. The specific capacitances (C<sub>s</sub>) were first evaluated from CV using the equation [18].

$$C_s = \frac{\int i dV}{2 V_s m \Delta V} \text{ (F/g)} \quad (2)$$

where

C<sub>s</sub> = Specific Capacitance

i = Current in (A)

V = Potential in CV Test (V)

V<sub>s</sub> = Scan rate (V/s)

m = Mass of active Material (g)

ΔV = Potential Window (V)

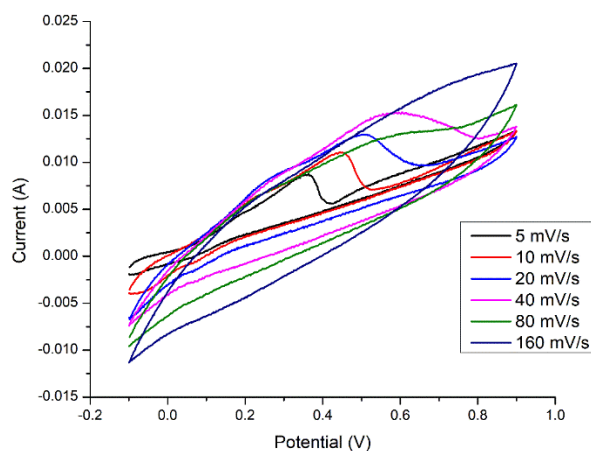


**Figure 10:** CV curves for starch-PANI composite at various scan rates (5, 10, 20, 40, 80 and 160 mV/s)

The specific capacitance for starch-PANI electrode calculated using the CV curves was 499.5, 262.5 and 138.10 F/g at scan rates of 5, 10 and 20 mV/s respectively. It can be seen that specific capacitance values decrease with an increase in scan rate, which indicates that high specific capacitance at a lower scan rate. Several conventional methods were synthesized the combination of PANI with carbon materials for electrochemical studies are mention in the introduction. But this work gives the maximum specific capacitance of starch-PANI is 499.5 F/g at 5 mV/s, which is greater than previously reported pure PANI, G-PANI and SDAS-PANI with their specific capacitances were 237, 379 and 433 F/g, respectively [51].

### 3.6.2 Galvanostatic Charge-Discharge (GCD)

The specific capacitances were also estimated by the galvanostatic charge-discharge (GCD) analysis. The GCD curves of starch-PANI at current densities of 0.5, 1 and 2 A/g are shown in Fig. 11. The synergistic effect between double layer capacitance and pseudocapacitance an obvious discharge pattern can be observed at the charge-discharge process, corresponding to starch and PANI [4]. The  $C_s$  values can be estimated using the below formula [52].

$$C_s = \frac{I \times \Delta t}{m \times \Delta V} \quad (3)$$

where

$C_s$  = Specific Capacitance (F/g)

$I$  = Discharge Current in (A)

$\Delta t$  = Discharge Time in (s)

$m$  = Mass of active Material (g)

$\Delta V$  = Potential Window (V)

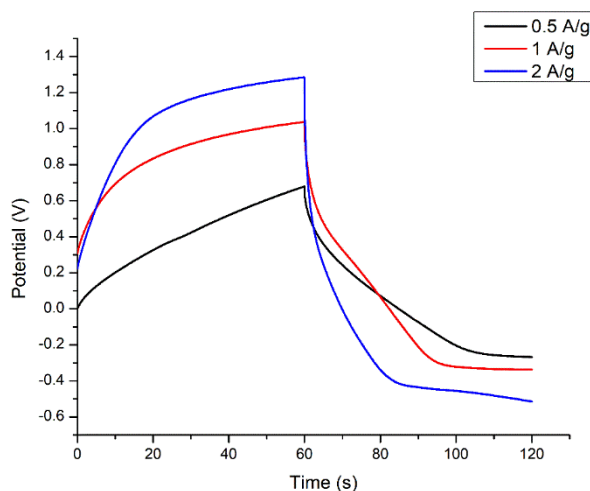


**Figure 11:** GCD curves of starch-PANI composite at different current densities (0.5, 1 and 2 A/g)

The  $C_s$  of the starch-PANI electrode evaluated by GCD curves were 66.5, 48 and 31.5 F/g at current densities of 2, 1 and 0.5 A/g respectively using GCD. Due to the pseudo capacitance behavior the resulting curves are triangular in shape. The GCD and CV curves are different due to the shape of GCD curves are not perfect and few errors in the calculation of specific capacitance by the discharge current and potential window. By comparing both the methods CV results are more precise values and the comparative analysis purpose GCD results are calculated.

Generally, a real electrochemical cell does not similar to an electrochemical cell. In a real electrochemical cell, the working electrode is keep at a relative distance to the reference electrode. Which indicates that uncompensated resistance cannot avoid totally. So, such resistance leads to voltage drop in

the electrochemical cell is known as IR drop. Even some cases low uncompensated resistance gives the higher voltage drop when the current is passed.

The following approaches can be used to avoid or minimize the IR drop.

- Higher conductivity electrolyte provides benefits that reduces the total resistances of the solution.
- The size of the working electrode is reduced, then it generates small amount of current which decrease the IR drop and the working electrode generates the total current depends on the surface area.
- The preliminary function of Luggin capillary is that which help in reduces the distance between the working electrode and the reference electrode and it also reduces uncompensated resistance.
- The positive feedback that generated most of recent potentiostats and also that effects the reduction of uncompensated resistance. In that case, IR compensation switch is ON during the operation of instrument.

### 3.6.3 Electrochemical Impedance Spectroscopy (EIS)

The EIS data were determined using the Nyquist plot. The conductivity of the electrode was analyzed by using EIS. EIS plot for starch-PANI composite is presented in Fig. 12. The Nyquist curve shows semicircle in the high frequency region and the finite slope of the straight line in the low frequency region. The curves, which are generally, shown in the shape of small semicircles, shows both the resistive and capacitive properties of the charge transport phenomenon [53]. The Nyquist plot for starch-PANI nanocomposite electrode was analyzed from 0.1 Hz to 100 kHz was frequency range and 5 mV was voltage amplitude with SCE as reference electrode. Nyquist plot of starch-PANI composite electrode material shows small semicircle and different slope lines, which indicate that starch-PANI composite electrode material, has the characteristic of apseudo capacitor and a double layer capacitor. Thus, starch-PANI nanocomposite electrode material exhibits excellent capacitive performance [54].

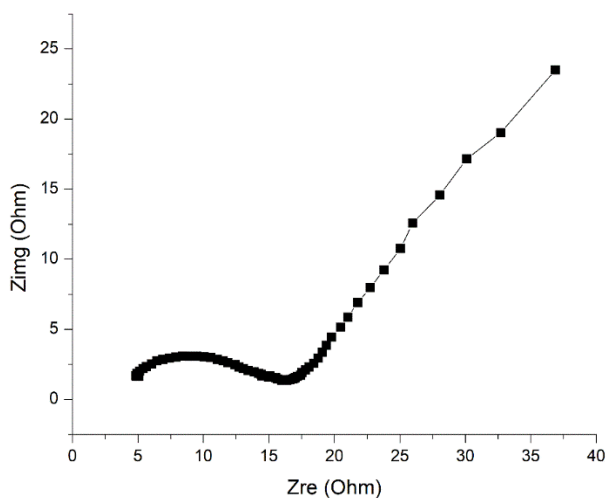


**Figure 12:** EIS Spectra of starch-PANI nanocomposite

## 4 Conclusion

In summary, starch coated with PANI nanocomposite has been synthesized by ultrasound assisted method. Aniline was polymerized on the conductive surface of starch granules in the presence of CTAB. APS was used as an initiator for polymerization. The specific capacitance was mainly contributed from the pseudo capacitance from the starch-PANI nanocomposite. The structural parameters, functional groups and morphology of the synthesized nanocomposite were studied in detail. The starch-PANI

nanocomposite was characterized by XRD, FT-IR, Raman, XPS and TEM. The electrochemical studies of the nanocomposite calculated by using CV, GCD and EIS. The starch coated with PANI (starch-PANI) composite electrode shown the maximum specific capacitance of 499.5 F/g at a scan rate of 5 mV/s. The starch-PANI blend has shown promising electrochemical performance and can be used as a reliable, biodegradable supercapacitor electrode.

**Acknowledgment:** This work was supported by the National Institute of Technology, Warangal (NITW) through the Technical Education Quality Improvement Program (TEQIP), MHRD.

## References

1. Jin, Y., Jia, M. (2015). Design and synthesis of nanostructured Graphene-SnO<sub>2</sub>-Polyaniline ternary composite and their excellent supercapacitor performance. *Colloids Surfaces A Physicochemistry Engineering. Asp*, 464, 17-25.
2. Ezeigwe, E. R., Tan, M. T., Khiew, P. S., Siong, C. W. (2015). Onestep green synthesis of Graphene-ZnO nanocomposites for Ec capacitors. *Ceramic International*, 41, 715-724.
3. González, A., Goikolea, E., Barrena, J. A., Mysyk, R. (2016). Review on supercapacitors: technologies and materials. *Renewable & Sustainable Energy Reviews*, 58, 1189-1206.
4. Gnana, B., Raj, S., Nair, R., Ramprasad, R., Asiri, A. M. et al. (2015). Ultrasound assisted synthesis of Mn<sub>3</sub>O<sub>4</sub> nanoparticles anchored graphene nanosheets for supercapacitor applications. *Electrochimica Acta*, 156, 127-137.
5. Iro, Z. S., Subramani, C., Dash, S. S. (2016). A brief review on electrode materials for supercapacitor. *International Journal of Electrochemical Science*, 11, 10628-10643.
6. Wu, M., Ai, P., Tan, M., Jiang, B., Li, Y. et al. (2014). Synthesis of starch-derived mesoporous carbon for electric double layer capacitor. *Chemical Engineering Journal*, 245, 166-172.
7. Pang, L., Zou, B., Zou, Y., Han, X., Cao, L et al. (2016). A new route for the fabrication of corn starch-based porous carbon as electrochemical supercapacitor electrode material. *Colloids Surfaces A Physicochemistry Engineering Asp*, 504, 26-33.
8. Liang, C., Bao, J., Li, C., Huang, H., Chen, C. et al. (2017). One-dimensional hierarchically porous carbon from biomass with high capacitance as supercapacitor materials. *Microporous Mesoporous Mater*, 251, 77-82.
9. Ruibin, Q., Zhongai, H., Yuying, Y., Zhimin, L., Ning, A. et al. (2015). Monodisperse carbon microspheres derived from potato starch for asymmetric supercapacitors. *Electrochimica Acta*, 167, 303-310.
10. Deng, L., Young, R. J., Kinloch, I. A., Abdelkader, A. M. et al. (2013). Supercapacitance from cellulose and carbon nanotube nanocomposite fibers. *ACS Applied Materials & Interfaces*, 5, 9983-9990.
11. Mo, Z. L., Zhao, Z. L., Chen, H., Niu, G. P., Shi, H. F. (2009). Heterogeneous preparation of cellulose-polyaniline conductive composites with cellulose activated by acids and its electrical properties. *Carbohydrate Polymers*, 75(4), 660-664.
12. Srivastav, S., Tammela, P., Brandell, D., Sjödin, M. (2015). Understanding ionic transport in polypyrrole/nanocellulose composite energy storage devices. *Electrochimica Acta*, 182, 1145-1152.
13. Gui, Z., Zhu, H., Gillette, E., Han, X., Rubloff, G. W. et al. (2013). Natural cellulose fiber as substrate for supercapacitor. *ACS Nano*, 7, 6037-6046.
14. Ma, T., Chang, P. R., Zheng, P., Ma, X. (2013). The composites based on plasticized starch and graphene oxide/reduced graphene oxide. *Carbohydrate Polymers*, 94, 63-70.
15. Cuong, N. V., Hieu, T. Q., Thien, P. T., Vu, L. D., Tan, L. Van. (2017). Reusable starch-graft-polyaniline/Fe<sub>3</sub>O<sub>4</sub> composite for removal of textile dyes. *Rasayan Journal of Chemistry*, 10, 1446-1454.
16. Huang, H., Yao, J., Chen, H., Zeng, X., Chen, C. et al. (2016). Facile preparation of halloysite/polyaniline nanocomposites via in situ polymerization and layer-by-layer assembly with good supercapacitor performance. *Journal of Material Science*, 51, 4047-4054.
17. Yang, C., Liu, P., Zhao, Y. (2010). Preparation and characterization of coaxial halloysite/polypyrrole tubular nanocomposites for electrochemical energy storage. *Electrochimica Acta*, 55, 6857-6864.

18. Li, K., Liu, X., Chen, S., Pan, W., Zhang, J. (2018). A flexible solid-state supercapacitor based on graphene/polyaniline paper electrodes. *Journal of Energy Chemistry*, 1-8.
19. Gautam, V., A, Srivastava, K., Singh, P. V., Yadav, L. (2015). Preparation and characterization of polyaniline, multiwall carbon nanotubes, and starch bionanocomposite material for potential bioanalytical applications. *Polymer Composites*, 1-11.
20. Aydinli, A., Yuksel, R., Unalan, H. E. (2018). Vertically aligned carbon nanotube-polyaniline nanocomposite supercapacitor electrodes. *International Journal of Hydrogen Energy*, 1-9.
21. Sivaraman, P., Rath, S. K., Hande, V. R., Thakur, A. P., Patri, M. et al. (2006). All-solid-supercapacitor based on polyaniline and sulfonated polymers. *Synthetic Metals*, 156, 1057-1064.
22. Kim, B. C., Kwon, J. S., Ko, J. M., Park, J. H., Too, C. O. et al. (2010). Preparation and enhanced stability of flexible supercapacitor prepared from nafion/polyaniline nanofiber. *Synthetic Metals*, 160, 94-98.
23. Prasad, K. R., Munichandraiah, N. (2002). Fabrication and evaluation of 450 F electrochemical redox supercapacitors using inexpensive and high-performance, polyaniline coated, stainless-steel electrodes. *Journal of Power Sources*, 112, 443-451.
24. Sharma, R. K., Rastogi, A. C., Desu, S. B. (2008). Pulse polymerized polypyrrole electrodes for high Energy density electrochemical supercapacitor. *Electrochemistry Communications*, 10, 268-272.
25. Ramya, R., Sivasubramanian, R., Sangaranarayanan, M. V. (2013). Conducting polymers-based electrochemical supercapacitors progress and prospects. *Electrochimistry Acta*, 101, 109-129.
26. Sowmya, M. S. (2018). Multilayered electrode materials based on polyaniline/activated carbon composites for supercapacitor applications. *International. Journal of Hydrogen Energy*, 43, 4067-4080.
27. Eftekhari, A., Li, L., Yang, Y. (2017). Polyaniline supercapacitors. *Journal of Power Sources*, 347, 86-107.
28. Lee, T., Yun, T., Park, B., Sharma, B., Song, H. K. et al. (2012). Hybrid multilayer thin film supercapacitor of graphene nanosheets with polyaniline: importance of establishing intimate electronic contact through nanoscale blending. *Journal of Material and Chemistry*, 22, 21092-21099.
29. Hu, Z. A., Xie, Y. L., Wang, Y. X., Mo, L. P., Yang, Y. Y. et al. (2009). Polyaniline/SnO<sub>2</sub> nanocomposite for supercapacitor applications. *Material Chemistry and Physics*, 114, 990-995.
30. Ni, W., Wang, D., Huang, Z., Zhao, J., Cui, G. (2010). Fabrication of nanocomposite electrode with MnO<sub>2</sub> nanoparticles distributed in polyaniline for electrochemical capacitors. *Material Chemistry and Physics*, 124, 1151-1154.
31. Shen, J., Yang, C., Li, X., Wang, G. (2013). High-performance asymmetric supercapacitor based on nano-architected polyaniline/graphene/carbon nanotube and activated graphene electrodes. *ACS Applied Material and Interfaces*, 5, 8467-8476.
32. Wu, Q., Chen, M., Wang, S., Zhang, X., Huan, L. et al. (2016). Preparation of sandwich-like ternary hierarchical nanosheets manganese dioxide/polyaniline/reduced graphene oxide as electrode material for supercapacitor. *Chemistry Engineering Journal*, 304, 29-38.
33. Lukaszewicz, M., Ptaszek, P., Ptaszek, A., Bednarz, S. (2014). Polyaniline-starch blends: synthesis, rheological, and electrical properties. *Starch/Staerke*, 66, 1-12.
34. Zareh, E. N., Moghadam, P. N., Azariyan, E., Sharifian, I. (2011). Conductive and biodegradable polyaniline/starch blends and their composites with polystyrene. *Iranian Polymer Journal*, 20, 319-328.
35. Caupin, F., Herbert, E. (2006). Cavitation in water: a review. *Comptes Rendus Physique*, 7, 1000-1017.
36. Vinodgopal, K., He, Y., Ashokkumar, M., Grieser, F. (2006). Sonochemically prepared platinum-ruthenium bimetallic nanoparticles. *Journal of Physics and Chemistry B*, 110, 3849-3852.
37. Wu, C. W., Mosher, B. P., Zeng, T. (2006). Rapid synthesis of gold and platinum nanoparticles using metal displacement reduction with sonomechanical assistance. *Chemistry and Material*, 18, 2925-2928.
38. Zhang, Y., Wang, X., Zeng, L., Song, S., Liu, D. (2012). Green and controlled synthesis of Cu<sub>2</sub>O-graphene hierarchical nanohybrids as high-performance anode materials for lithium-ion batteries via an ultrasound assisted approach. *Dalton Transactions*, 41, 4316-4319.
39. Zhu, X., Zhu, Y., Murali, S., Stoller, M. D., Ruoff, R. S. (2011). Nanostructured reduced graphene oxide/Fe<sub>2</sub>O<sub>3</sub> composite as a high-performance anode material for lithium ion batteries. *ACS Nano*, 5, 3333-3338.
40. Majumdar, D., Bhattacharya, S. K. (2017). Sonochemically synthesized hydroxy-functionalized graphene-

- MnO<sub>2</sub> nano composite for supercapacitor applications. *Journal of Applied Electrochemistry*, 47, 789-801.
41. Ghasemi, S., Hosseini, S. R., Boore-talari, O. (2018). Ultrasonics-sonochemistry sonochemical assisted synthesis MnO<sub>2</sub>/RGO nanohybrid as effective electrode material for supercapacitor. *Ultrason.-Sonochemistry*, 40, 675-685.
  42. Safarifard, V., Morsali, A. (2015). Applications of ultrasound to the synthesis of nanoscale metal-organic coordination polymers. *Coordination Chemistry Reviews*, 292, 1-14.
  43. Prasad, J., Banerjee, S., Kumar, B., Kumar, A. (2010). Biocompatible novel starch/polyaniline composites: characterization, anti-cytotoxicity and antioxidant activity. *Colloids Surfaces B Biointerfaces*, 81, 158-164.
  44. Pouget, J. P., Jdzefowicz, M. E., Epstein, A. J., Tang, X., Macdiarmid, A. G. (1991). X-Ray structure of polyaniline. *Macromolecules*, 24, 779-789.
  45. Yadagiri, M., Ramakrishna, S., Ravi, G., Suresh, P., Sreenu, K. et al. (2015). Preparation, characterization and photocatalytic studies of Cr<sub>2</sub>(MoO<sub>4</sub>)<sub>3</sub> and nitrogen-doped Cr<sub>2</sub>(MoO<sub>4</sub>)<sub>3</sub>. *Chemical Technology*, 9, 391-399.
  46. Musa, M. B., Yoo, M. J., Kang, T. J., Kolawole, E. G., Ishiaku, U. S. et al. (2013). Characterization and thermomechanical properties of thermoplastic potato starch. *Journal of Engineering Technology*, 2, 9-16.
  47. Liu, H., Hu, X. B., Wang, J. Y., Boughton, R. I. (2002). Structure, conductivity, and thermopower of crystalline polyaniline synthesized by the ultrasonic irradiation polymerization method. *Macromolecules*, 35, 9414-9419.
  48. Janaki, V., Vijayaraghavan, K., Oh, B. T., Lee, K. J., Muthuchelian, K. et al. (2012). Starch/polyaniline nanocomposite for enhanced removal of reactive dyes from synthetic effluent. *Carbohydrate Polymers*, 90, 1437-1444.
  49. Shi, Z., Zang, S., Jiang, F., Huang, L., Lu, D. et al. (2012). In situ nano-assembly of bacterial cellulose-polyaniline composites. *RSC Advances*, 2, 1040-1046.
  50. Wang, H., Zhu, E., Yang, J., Zhou, P., Sun, D. et al. (2012). Bacterial cellulose nano fiber-supported polyaniline nanocomposites with flake-shaped morphology as supercapacitor electrodes. *Journal of Physical Chemistry C*, 116, 13013-13019.
  51. Wu, W., Li, Y., Yang, L., Ma, Y., Pan, D. et al. (2014). A facile one-pot preparation of dialdehyde starch reduced graphene oxide/polyaniline composite for supercapacitors. *Electrochimica Acta*, 139, 117-126.
  52. Yang, Y., Xi, Y., Li, J., Wei, G., Klyui, N. I. et al. (2017). Flexible supercapacitors based on polyaniline arrays coated graphene aerogel electrodes. *Nanoscale Research Letters*, 12, 1-9.
  53. Qaiser, A. A., Hyland, M. M., Patterson, D. A. (2011). Surface and charge transport characterization of polyaniline-cellulose composite membranes. *Journal of Physical Chemistry B*, 115, 1652-1661.
  54. Jin, Z., Ren, X., Qin, C., Li, B., Quan, S. et al. (2011). Hybrid supercapacitors based on polyaniline and activated carbon composite electrode materials. *Pigment & Resin Technology*, 40, 235-239.
  55. Htut, K. Z., Kim, M., Lee, E., Lee, G., Baeck, S. H. et al. (2017). Biodegradable polymer-modified graphene/polyaniline electrodes for supercapacitors. *Synthetic Metals*, 227, 61-70.
  56. Aydinli, A., Yuksel, R., Unalan, H. E. (2018). Vertically aligned carbon nanotube e Polyaniline nanocomposite supercapacitor electrodes. *International Journal of Hydrogen Energy*, 1-9.